LVRT-Compliant Control of Three-Phase Grid-Connected Module-Integrated Converters Using Chaos Game Optimization

MD Samiul Alam, MD Arif Hossain, Fahad S. Al-Ismail, Abdulaziz Qwbaiban, Mohammad A. Abido
Department of Electrical Engineering
King Fahd University of Petroleum and Minerals
Dhahran, Saudi Arabia
g202426860@kfupm.edu.sa, g202426040@kfupm.edu.sa, fsalismail@kfupm.edu.sa, qwbaiban@kfupm.edu.sa, mabido@kfupm.edu.sa

***Abstract*—As PV penetration rises, grid-connected PV plants can adversely affect grid stability during disturbances. This paper presents a reset-free, Chaos Game Optimization (CGO)-based maximum power point tracker for a 5-MW PV plant interfaced through a boost converter and a grid-connected inverter. The CGO block is co-designed with a phase-locked loop (PLL)-synchronized dq-axis current controller. The inverter enforces current limiting with reactive power priority during voltage sags. MATLAB/Simulink results show 99.9% tracking efficiency and a regulated 600-V DC link. Under single-line-to-ground and three-phase faults cleared at a specific time, currents remain bounded, the PLL stays locked, and post-fault variables return to their pre-fault setpoints with prompt MPPT resumption. Low-voltage ride-through (LVRT) capability is demonstrated, and the control strategy is validated in MATLAB/Simulink. The approach uses few tuning parameters and constant-time computation and is suitable for real-time deployment in utility-scale PV systems.**

***Index Terms*—Maximum Power Point Tracking (MPPT), Chaos-Game Optimization (CGO), Grid-Connected Inverter, Low-Voltage Ride-Through (LVRT), Phase-Locked Loop (PLL).**

I. Introduction

The rapid growth of grid-tied photovoltaic (PV) systems has led to extensive research on efficient converter topologies and advanced control strategies, with particular attention to module-integrated converters (MICs) that offer scalability, improved reliability, and the elimination of single points of failure. However, the integration of PV systems into the utility grid introduces several power-quality challenges, including voltage harmonics, voltage sags and swells, and frequency deviations [1]. The widespread adoption of nonlinear loads, such as compact fluorescent lamps (CFLs), variable-speed drives, and power-electronic-interfaced converters, further exacerbates these issues by distorting voltage and current waveforms, thereby contributing to harmonic pollution in grid-tied PV (GTPV) systems. In addition, unbalanced voltage sags and swells give rise to fluctuations in the active and reactive power injected into the grid, resulting in undesirable ripples [2]. To ensure reliable and stable operation of GTPV systems, it is essential to suppress grid-current harmonics and mitigate power ripples. These persistent challenges have motivated significant research efforts aimed at enhancing the power quality of GTPV systems by developing effective harmonic-suppression and ripple-reduction strategies.

In [3], a repetitive-learning-based phase-locked loop (PLL) is introduced to enhance the power quality of grid-connected DC microgrids under distorted voltage conditions. However, this approach assumes PV sources are ideal DC voltage inputs, thereby neglecting maximum power point (MPP) extraction. Furthermore, the mitigation of active and reactive power ripples remains limited, indicating scope for further improvement. The system model of a three-phase MIC in [4] is typically formulated in the synchronous dq reference frame, allowing active and reactive power to be directly regulated using discrete prediction models of grid currents and converter states. In this context, finite-control-set model predictive control (FCS-MPC) has emerged as a powerful method, directly selecting optimal switching states without the need for modulation and resulting in fast transient response, reduced complexity, and robust performance under grid disturbances. However, conventional MPC relies on proportional–integral (PI) regulation of the DC-link current for reference generation, which limits adaptability under nonlinear operating conditions [5]. To address this, recent research has explored soft-computing methods for both maximum power point tracking (MPPT) and adaptive inverter control. Furthermore, metaheuristic algorithms such as particle swarm optimization (PSO), grey wolf optimization (GWO), and ant colony optimization (ACO) have been shown to outperform conventional MPPT techniques in scenarios with partial shading and multiple local maxima.

Hamrouni et al. [6] broadly categorize the control mechanisms of grid-connected PV systems into two groups: PLL-based and non-PLL-based methods. The authors argue that "advanced AI" and "soft-computing controllers" outperform conventional control strategies. While that work does not enumerate specific metaheuristics, it clearly motivates intelligent optimization as a response to variable irradiance and tempera-

Inter-disciplinary Research Center for Sustainable Energy Systems (IRC-SES), King Fahd University of Petroleum & Minerals (KFUPM), Saudi Arabia,

979-8-3315-8138-1

ture, grid-integration demands, and the need for robust tracking and regulation in a changing operating environment. Moreover, metaheuristics enable controllers to adapt to disturbances and nonlinearities [7]. The authors of [8] investigated the optimal sizing and placement of PV systems to improve voltage profiles and reduce losses in the grid. A large body of work has examined grid-connected and stand-alone PV systems [9]. It should be noted that conventional MPPT algorithms can fail when PV arrays operate under partial-shading conditions. To improve the operating efficiency of large-scale solar PV systems, a more efficient soft-computing technique should be employed to optimize the global MPP. The proposed intelligent control strategy automatically synchronizes a VSI to the grid without a dedicated synchronization system. Along with grid-current harmonic mitigation and power-oscillation elimination, efficient and fast MPP operation of the PV array is ensured by incorporating a new MPPT controller.

II. Problem Statement

Conventional grid-tied module-integrated converters (MICs) are predominantly based on single-phase voltage-source inverters (VSIs), which require additional boosting stages, involve complex modulation techniques, and exhibit limitations with respect to low-voltage ride-through (LVRT) capability [10]. Existing LVRT enhancement methods primarily rely on proportional–integral (PI) regulators and modulation-based control, which suffer from slower transient response and limited adaptability to system nonlinearities [11]. Therefore, there is a critical need for a control framework that can directly handle system nonlinearities, eliminate dependence on conventional modulation, and guarantee LVRT performance in PV-based MICs for large-scale PV applications.

These limitations create an opportunity for hybrid soft-computing techniques. Methods such as fuzzy logic, adaptive neuro-fuzzy inference systems (ANFIS), and artificial neural networks (ANNs) can replace or augment PI-based reference generation by providing adaptive, nonlinear mappings that respond more effectively to rapid irradiance and temperature fluctuations. Metaheuristic algorithms such as particle swarm optimization (PSO) and grey wolf optimization (GWO) have been employed in previous work to optimize cost-function weights or dynamically tune controller parameters, ensuring a better trade-off among power-tracking accuracy, switching frequency, and harmonic performance. Furthermore, newly developed metaheuristic approaches, such as CGO for MPPT or PID-tuned cost functions for inverter control, can extend the framework to simultaneously maximize PV energy extraction, reduce oscillations near the MPP, and guarantee LVRT-compliant reactive-current injection during faults. Fig. 1 shows the proposed system model. By embedding these soft-computing techniques within the existing framework, the controller can achieve higher efficiency, improved adaptability under nonlinear and uncertain conditions, and enhanced compliance with evolving grid codes, thereby addressing shortcomings of the baseline predictive control strategy.

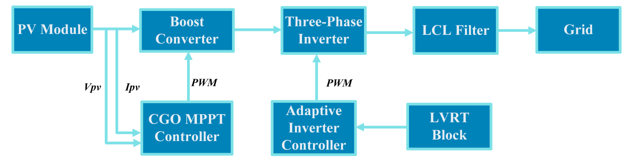

Fig. 1. Proposed intelligent control approach for a three-phase single-stage grid-tied PV module-integrated converter

$$\max_{V_{\text{ref}}} P(V) = V I \tag{1}$$

Here $V_{\min} \le V_{\text{ref}} \le V_{\max}$, and $|\Delta V_{\text{ref}}| \le \dot{V}_{\max} T_s$.

where T_s is the MPPT update period and $\dot{V}_{\max}$ is a time-normalized slew limit used to suppress DC-bus disturbances.

III. Methodology

A 5 MW grid-connected photovoltaic (PV) system was designed, simulated, and analyzed using control approaches for maximum power point tracking (MPPT) and adaptive inverter regulation. A recently evolved chaos game optimization (CGO) algorithm is used, among other soft-computing techniques, to improve accuracy and convergence. The adaptive inverter controller maintains in-phase voltage and current, provides reactive-power compensation, mitigates harmonics, and ensures grid synchronization during low-voltage ride-through (LVRT) conditions portrayed by the three-phase fault block. The system architecture consists of a PV array, a DC–DC boost converter for voltage regulation, a three-phase voltage-source inverter (VSI) for DC–AC conversion, a three-phase fault block that implements short circuits between any phase and ground, and an LCL filter for harmonic suppression prior to grid interconnection. System parameters are summarized in Tables I and II, and the boost-converter inductance L and capacitance C values were computed in MATLAB/Simulink. The overall system configuration is illustrated in Fig. 2.

TABLE I
PV Module Parameters

Parameter	Value
V_{mp}	29 V
I_{mp}	7.35 A
V_{oc}	36.3 V
I_{sc}	7.84 A
PV Modules in Series, M_S	11
PV Number of Strings, M_P	2132
Maximum Power at PV Array, P_{maxPV}	5 MW

A. Chaos Game Optimization (CGO) MPPT

This work employs a Chaos Game Optimization (CGO)-based MPPT to enhance both global search and local fine-tuning within a single stage. CGO generates candidate operating voltages by contracting toward multiple attractors inside a safe envelope $[V_{\min}, V_{\max}]$, using an adaptive contraction factor and a shrinking search radius to balance exploration

979-8-3315-8138-1

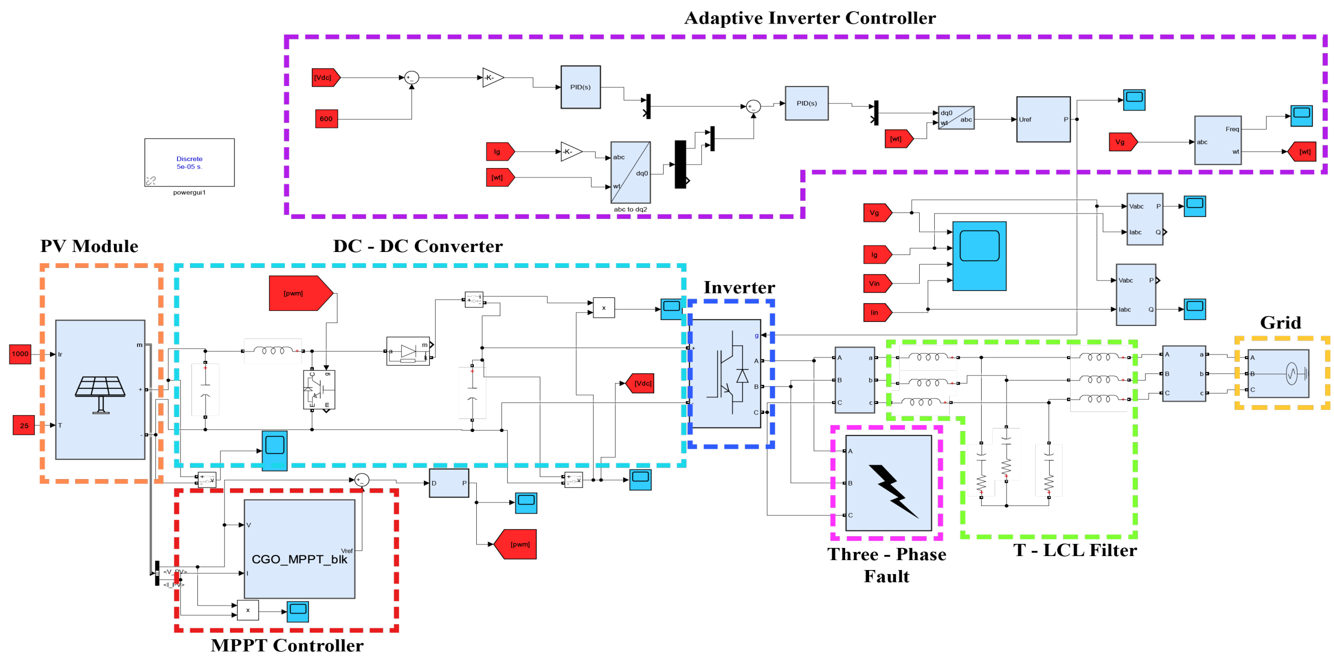

Fig. 2. Functional block diagram of the proposed CGO-MPPT-based PV-integrated grid-tied inverter.

TABLE II
BOOST CONVERTER PARAMETERS

Parameter	Value
Nominal Input Voltage, V_{in}	329 V
Input Capacitance, C_{pv}	0.0650 F
Input Inductance, L_b	9.5316×10^{-5} H
Inductor Internal Resistance, R_{Lb}	0.0720 Ω
Switching Frequency, f_s	10 kHz

and exploitation under changing irradiance and temperature conditions [12]. The measured power $P = VI$ is taken as the fitness, and the best candidate recenters the search, while a slope gate, which holds when $|\Delta P/\Delta V|$ is small, suppresses steady-state dithering and ripple [13]. Under partial shading, a re-expansion trigger restores the radius to regain global-search ability, after which it contracts again for fine-tuning. This single-stage CGO MPPT thus provides fast global convergence and low-ripple, steady-state operation on the 5 MW PV–boost platform, with few hyperparameters and straightforward real-time implementation.

$$V_{t+1} \;=\; \Pi_{[V_{\min},\,V_{\max}]}\Big(V_t \;+\; c_t\big(A_{k_t} - V_t\big) \;+\; \xi_t\Big) \tag{2}$$

$$\mathbf{x}_{t+1} \;=\; \mathrm{proj}_{\mathcal{X}}\Big(\mathbf{x}_t \;+\; c_t\big(\mathbf{a}_{k_t} - \mathbf{x}_t\big) \;+\; \boldsymbol{\xi}_t\Big) \tag{3}$$

Where A_{k_t} is a randomly selected attractor from the fixed set $A = \{A_1, \ldots, A_K\}$, $c_t \in [c_{\min}, c_{\max}]$ is the contraction factor, ξ_t is a small jitter, with $\rho_t > 0$, the current search radius and $\varepsilon \in (0, 1)$ a jitter fraction, $\mathrm{proj}_{\mathcal{X}}$ denotes projection onto the safe domain, i.e., the interval $[V_{\min}, V_{\max}]$ in the scalar case or the feasible set $\mathcal{X}$ in the vector case.

B. Proposed Technique for Three-Phase Inverter Control

The grid-side converter employs a cascaded, synchronous-reference-frame current-regulated architecture locked to the utility via a phase-locked loop (PLL). Measured three-phase currents and voltages are mapped to the dq frame using the PLL angle; an outer DC-link voltage controller shapes active-power flow by producing the d-axis current reference, while the q-axis reference is set to meet reactive-power objectives and unity power factor in the baseline case. Inner dq current controllers with cross-coupling compensation and grid-voltage feedforward track these references and generate dq voltage commands that are transformed back to abc and passed to a space-vector modulator to synthesize the inverter gating signals. The synthesized voltages are applied through the LCL filter to the point of common coupling, with damping and saturation to ensure stability under grid-strength variations. Bandwidth separation is enforced: the current loops are fastest, the DC-link loop is slower, and MPPT is slowest, ensuring DC-link regulation, power-factor control, and ripple suppression without interaction.

$$e_d = i_d^{\star} - i_d \tag{4}$$

$$e_q = i_q^{\star} - i_q \tag{5}$$

Here, e_d and e_q are the d- and q-axis current–tracking errors used by the inner current controllers, i_d and i_q are the measured converter (grid) currents expressed in the synchronous dq frame, and $i_d^{\star}$ and $i_q^{\star}$ are the corresponding current references supplied by the outer loops, for e.g., the DC-link voltage regulator for $i_d^{\star}$ and the power-factor regulator for $i_q^{\star}$.

979-8-3315-8138-1

$$v_d^\star = v_{g,d} + k_{p,d}\, e_d + k_{i,d} \int e_d \, \mathrm{d}t \; - \; \omega\, L\, i_q, \qquad (6)$$

$$v_q^\star = v_{g,q} + k_{p,q}\, e_q + k_{i,q} \int e_q \, \mathrm{d}t \; + \; \omega\, L\, i_d. \qquad (7)$$

Where, $v_d^\star$ and $v_q^\star$ are the commanded inverter voltage references in the synchronous dq frame, $v_{g,d}$ and $v_{g,q}$ are the grid (PCC) voltage components used for feedforward, $k_{p,d}$, $k_{i,d}$, $k_{p,q}$, and $k_{i,q}$ are the proportional and integral gains of the d- and q-axis current controllers, and L is the per-phase filter inductance or the effective inductance seen by the controller.

IV. Results and Analysis

The PV array feeds a DC–DC converter to maintain a constant DC-link voltage V_{dc}. The DC-link capacitance is set by two criteria: buffering the worst PV–AC power mismatch over the fault window and limiting the 2ω ripple under imbalance. Both are computed from the assumed fault duration and the allowed V_{dc} band. The proposed system is evaluated by time-domain simulation under nominal operation and a balanced three-phase LVRT fault at the point of common coupling (PCC). In steady state, CGO-MPPT tracks the MPP with low ripple within the enforced voltage envelope, the DC-link regulator holds 600 V, and synchronous dq current control produces near-sinusoidal grid currents. During the fault, the LVRT logic limits current, prioritizes reactive support, and curtails active power to keep the DC link bounded while the PLL remains locked. After clearance, the currents and DC-link voltage return smoothly to their setpoints, and CGO resumes MPP tracking without hunting. Overall, the results demonstrate compliant ride-through and rapid post-fault restoration for the 5 MW grid-following inverter. Under both the single-line-to-ground and three-phase faults shown in Figs. 3 and 4, the inverter experiences the expected voltage sag, engages current limiting to keep phase currents bounded, and restores nominal waveforms rapidly after clearance. Figure 5 illustrates the grid-side voltage sag and the maintained, bounded grid currents throughout the ride-through window, with a smooth return to pre-fault levels after clearance. Parametric tests carried across fault durations identified a critical window near 0.66 seconds, beyond which the system loses stability, evidenced by growth in PLL phase error and DC-link divergence.

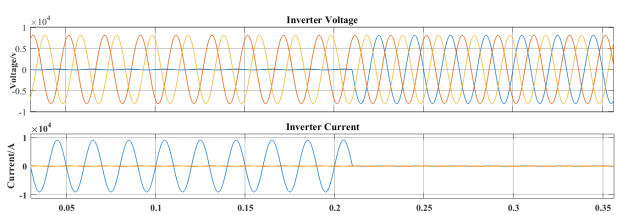

Fig. 3. Simulated waveforms of inverter voltage and inverter current during a single L-G fault cleared at 0.2s under STC.

Table III shows the proposed CGO method located the maximum power point at 4.99 MW, achieving 99.9 percent tracking efficiency with a convergence time of 0.6 seconds. TLBO and GWO reached the same power and efficiency, with convergence times of 0.9 seconds and 0.8 seconds, respectively. Adaptive PSO identified 4.94 MW and required

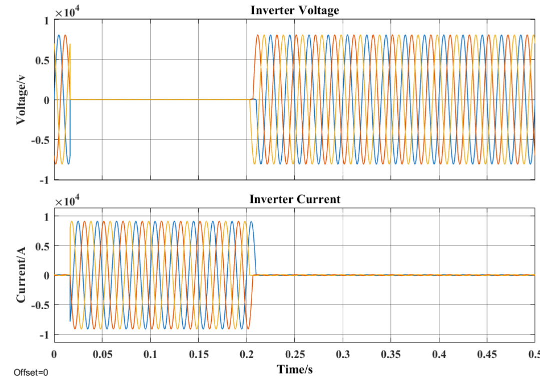

Fig. 4. Simulated waveforms of inverter voltage and inverter current during a three-phase-to-ground fault cleared at 0.2s under STC.

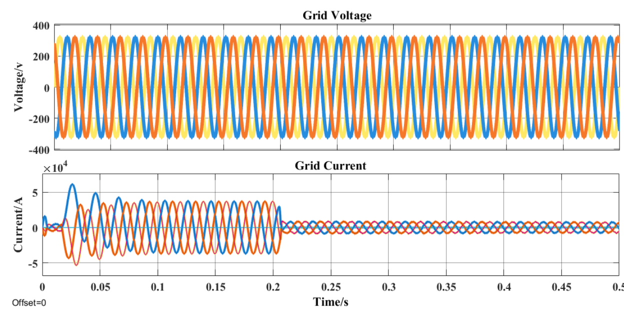

Fig. 5. Simulated waveforms of grid voltage and grid current during the LVRT.

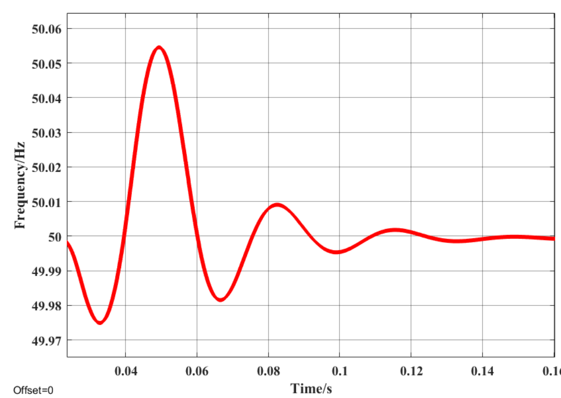

Fig. 6. Frequency oscillation during the three-phase fault.

TABLE III
Comparison of MPPT Algorithms

Parameter	**MPPT Algorithms**					
	P & O	**PSO**	**Adaptive PSO**	**TLBO**	**GWO**	**CGO**
T_s (s)	1.5	1.3	1.3	0.9	0.8	0.6
Power (MW)	4.64	4.88	4.94	4.96	4.96	4.99
η (%)	92.8	97.6	98.8	99.2	99.2	99.9

979-8-3315-8138-1

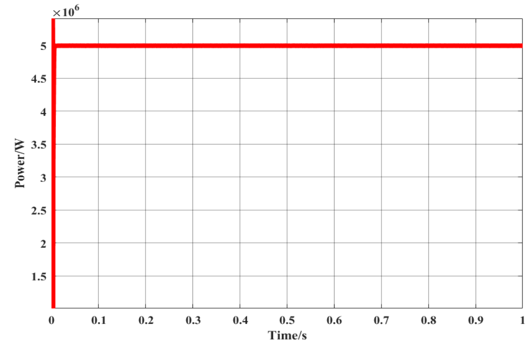

Fig. 7. MPP power output of 5MW PV module under CGO.

1.3 seconds to settle, slower than TLBO, GWO, and CGO. The classic PSO exhibited pronounced oscillations that increased losses and limited efficiency to 97.6 percent despite reaching the maximum power point, while P&O delivered lower power and efficiency. Fig. 6 illustrates the system frequency exhibits a lightly damped transient at fault inception: an initial dip to 49.98 Hz, a peak overshoot of 50.06 Hz corresponding to 0.12 percent of nominal at about 0.05 s, and settling within ±0.01 Hz of 50 Hz by 0.12 s without sustained oscillation. The findings demonstrate that the CGO method accurately tracks the MPP at $5\,\mathrm{MW}$ as shown in Fig. 7, achieving a tracking efficiency of 99.9%. The PV array output voltage is maintained at a constant level by the DC–DC converter. Furthermore, the active power delivered to the grid is regulated to remain constant. When irradiance drops, the grid power settles to the new MPP, as illustrated in Fig. 8.

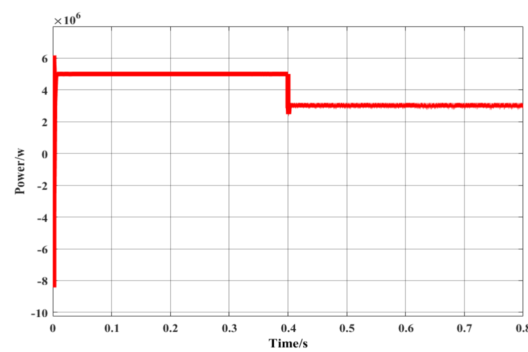

Fig. 8. Active power observed at the grid.

V. Conclusion

This paper presented a single-stage Chaos Game Optimization (CGO) MPPT integrated with a $5\,\mathrm{MW}$ PV–boost converter and a grid-connected inverter. Under matched irradiance ramps, partial shading, and LVRT sags, the reported metrics include tracking efficiency, settling time, V_{ref} ripple, PLL phase error, and peak current. Results indicate higher efficiency and lower ripple for CGO while respecting current limits. Time-domain studies under nominal operation and a severe LVRT event, modeled as a balanced three-phase fault at the PCC, show that the system rides through without loss of synchronism or controller windup; current limits are respected, reactive support is prioritized during the sag, the DC-link remains bounded, and post-fault variables return smoothly to their setpoints while CGO promptly recaptures the MPP. Overall, the results indicate that the proposed CGO MPPT and control architecture achieve stable, standards-compliant operation with rapid recovery and low ripple on a utility-scale PV plant. Future work will include hardware-in-the-loop (HIL) validation and field tests under partial-shading and weak-grid conditions.

Acknowledgment

The authors acknowledge the support provided by the Interdisciplinary Research Center for Sustainable Energy Systems (IRC-SES) and King Fahd University of Petroleum & Minerals (KFUPM) in Saudi Arabia for funding this work through Project number (INSE2514).

References

[1] S. Golestan, J. M. Guerrero, and J. C. Vasquez, "A pll-based controller for three-phase grid-connected power converters," *IEEE Transactions on Power Electronics*, vol. 33, no. 2, pp. 911–916, 2018.

[2] M. Ferrari, L. M. Tolbert, and E. C. Piesciorovsky, "Grid forming inverter with increased short-circuit contribution to address inverter-based microgrid protection challenges," *IEEE Open Journal of the Industrial Electronics Society*, vol. 5, pp. 481–500, 2024.

[3] N. Mohammed, H. Udawatte, W. Zhou, D. J. Hill, and B. Bahrani, "Grid-forming inverters: A comparative study of different control strategies in frequency and time domains," *IEEE Open Journal of the Industrial Electronics Society*, vol. 5, pp. 185–214, 2024.

[4] A. Hassan, O. Bass, and M. A. Masoum, "An improved genetic algorithm based fractional open circuit voltage mppt for solar pv systems," *Energies*, vol. 9, pp. 1535–1548, 2023.

[5] T. Li, Y. Li, S. Li, and W. Zhang, "Research on current-limiting control strategy suitable for ground faults in ac microgrid," *IEEE Journal of Emerging and Selected Topics in Power Electronics*, vol. 9, no. 2, pp. 1736–1750, 2021.

[6] N. Hamrouni, M. Jraidi, and A. Cherif, "New control strategy for 2-stage grid-connected photovoltaic power system," *Renewable Energy*, vol. 33, no. 10, pp. 2212–2221, 2008.

[7] F. Sadeque, M. Gursoy, and B. Mirafzal, "Grid-forming inverters in a microgrid: Maintaining power during an outage and restoring connection to the utility grid without communication," *IEEE Transactions on Industrial Electronics*, vol. 71, no. 10, pp. 11 796–11 805, 2024.

[8] S. K. V., D. G., and S. M. Sulthan, "Adaptive particle swarm optimization based improved modeling of solar photovoltaic module for parameter determination," *e-Prime – Advances in Electrical Engineering, Electronics and Energy*, vol. 8, p. 100621, 2024.

[9] L. Tarisciotti, A. Formentini, A. Gaeta, M. Degano, P. Zanchetta, and P. Wheeler, "Model predictive control for shunt active filters with fixed switching frequency," *IEEE Transactions on Industry Applications*, vol. 53, no. 1, pp. 296–304, 2017.

[10] V. Yaramasu, B. Wu, S. Alepuz, and S. Kouro, "Predictive control for low-voltage ride-through enhancement of three-level-boost and npc-converter-based pmsg wind turbine," *IEEE Transactions on Industrial Electronics*, vol. 61, no. 12, pp. 6832–6843, 2014.

[11] V. Yaramasu and B. Wu, "Model predictive decoupled active and reactive power control for high-power grid-connected four-level diode-clamped inverters," *IEEE Transactions on Industrial Electronics*, vol. 61, no. 7, pp. 3407–3416, 2013.

[12] M. Barakat, "Novel chaos game optimization tuned-fractional-order pid fractional-order pi controller for load-frequency control of interconnected power systems," *Protection and Control of Modern Power Systems*, vol. 7, no. 2, pp. 1–20, 2022.

[13] A. A. Mohamed, S. Kamel, M. H. Hassan, and J. L. Domínguez-García, "Optimal power flow incorporating renewable energy sources and facts devices: a chaos game optimization approach," *IEEE Access*, vol. 12, pp. 23 338–23 362, 2024.

979-8-3315-8138-1